Near −Optimization of Operating Conditions and Residence Time in Multi-zone Dryers for Polymer Coatings

ARTICLE *in* INDUSTRIAL & ENGINEERING CHEMISTRY RESEARCH · JANUARY 2009

Impact Factor: 2.59

2 AUTHORS:

Raj Kumar Arya
Thapar University
30 PUBLICATIONS **28** CITATIONS
SEE PROFILE

Madhu Vinjamur
Indian Institute of Technology Bombay
53 PUBLICATIONS **268** CITATIONS
SEE PROFILE

PROCESS DESIGN AND CONTROL

Near-Optimization of Operating Conditions and Residence Times in Multizone Dryers for Polymer Coatings

Raj K. Arya and Madhu Vinjamur*

Department of Chemical Engineering, IIT Bombay, Powai, Mumbai, India 400 076

Several polymeric coatings are dried by blowing jets of hot air on them from the top and bottom sides in multizone dryers. The goal of quickly removing solvent from a coating by manipulating air flow and temperature, together called operating conditions in this work, conflicts with the goal of producing blister-free coatings. Optimum operating conditions ensure both minimum residual solvent and no defects. Determining optimum conditions for multizone dryers is a difficult task with severe convergence problems. In this work, an easy method is developed to determine near-optimum operating conditions and residence times. The results indicate that the air flow on the top side should always be lower than or equal to that on the bottom side; the minimum residence time in first zone should be such that, toward the end, the solvent concentration starts to fall at the bottom. As long as the residence times are reasonably long, several different combinations of residence times in the second and subsequent zones nearly minimize residual solvent.

Introduction

Polymeric coatings such as photographic films, magnetic media, and synthetic fibers are produced by casting a layer of polymer solution, made by dissolving a polymer in a solvent, on a substrate; multiple layers can also be cast with a different polymer and solvent in each layer. The wet coatings are then dried, usually in multizone ovens or dryers, by blowing or impinging jets of hot air on them. The flow rate, temperature, and degree of solvent saturation of the air are the most important operating conditions, with the first two being more important than the third. In multizone dryers, the operating conditions generally change from one zone to another. These operating conditions are manipulated to achieve two goals: one is to remove the solvent(s) quickly, and the other is to dry the coatings without creating defects such as blisters.

Drying is the last and quality-controlling step in the production of polymer coatings; hence, coatings with defects lead to production losses. Because of poor choice of operating conditions, defects could be induced in the coatings: for example, internal gradients could develop, blisters could form, coatings could crack, phases could separate. Performing drying experiments at high air flows to mimic industrial dryers is a difficult task. Hence, mathematical modeling has been used extensively to describe the drying behavior of coatings.[1−8] Models have been verified to be accurate by comparing their predictions with data from weight-loss experiments[9−11] in the past and with concentration depth profiles in drying coatings more recently.[12,13] In this work, mathematical modeling has been used to find operating conditions that minimize residual solvent (solvent remaining in the coating at the end of drying) without generating blisters.

During the drying of coatings, solvent leaves only from the top, as the substrate is usually impermeable. The polymer moves only within the coating because it is nonvolatile at the temperatures at which the coating is dried. At every instant of time, a concentration gradient develops for the solvent, with its concentration being lowest at the top and highest at the bottom. A concentration gradient also forms for the polymer, but unlike for the solvent, the polymer's concentration is highest at the top and lowest at the bottom. As drying proceeds, the solvent concentration falls everywhere in the coating, and the polymer concentration increases. As the solvent concentration falls at the top, the diffusion coefficient, which is a strong function of concentration and temperature, falls sharply there.[14,15] Therefore, a steep concentration gradient of the solvent develops at the top to match the external flux of the solvent due to the air flow.

Cairncross[16] showed that, at any instant of time during drying, the bubble-point temperature can be estimated by equating the solvent partial pressure to the ambient pressure (usually 1 atm). Partial pressure equals vapor pressure multiplied by solvent activity, which can be estimated by Flory−Huggins theory. Solvent activity rises from the top to the bottom of the coating at all instants of time because of the increase in the solvent concentration from the top to the bottom. The vapor pressure, however, remains practically same through the coating thickness[17,18] because of the negligible change in the coating temperature from the top to the bottom. Therefore, the bubble-point temperature falls from the top to the bottom of the coating. The bubble-point temperature corresponding to the bottom of the coating is taken as the bubble-point temperature of the coating, because any temperature greater than it leads to blister formation.

Solvent concentration at the bottom of the coating does not drop from its initial value for a certain period of time during which the bubble-point temperature of the coating remains constant at the temperature corresponding to the initial solvent concentration. This duration is longer at lower air flows and temperatures and shorter at higher air flows and temperatures. As the solvent concentration at the bottom falls, the bubble-point temperature of the coating rises because of falling solvent activity at the bottom. However, the coating temperature rises to the air temperature as it is being heated from the top and the bottom. Cairncross[16] stated that blisters form when the coating

* To whom correspondence should be addressed. E-mail: madhu@che.iitb.ac.in. Fax: +91-22-2572 6895. Tel.: +91-22-2576 7218.

10.1021/ie900604f CCC: $40.75
Published on Web 10/01/2009

temperature exceeds the bubble-point temperature at any time during drying and showed that, at a given air temperature, blisters are more likely to be generated at higher air flows.

Intense operating conditions (i.e., high air flows and high temperatures) lead to higher rates of solvent removal but could generate blisters in the coatings. Mild conditions (i.e., low air flows and low temperatures) result in lower rates of solvent removal without creating blisters. Optimum conditions, which lie between intense and mild conditions, result in adequately high rates of solvent removal without inducing blisters. To enhance the drying speed without compromising the coating quality, dryers should be designed to operate at optimum conditions.

Cairncross et al.[5] used mathematical modeling to analyze the drying behavior of polymeric coatings in multizone dryers. They considered an existing industrial dryer and demonstrated that adjusting the operating conditions in each zone results in faster drying of the coating. They also showed that blisters are more likely to form in later zones—a fact confirmed by practicing engineers. Subzoning (i.e., dividing one zone into several zones) and applying a gradual rise in temperature in the subzones helps in achieving a higher rate of solvent removal. It was also illustrated that evaporative cooling decreases the rate of drying in the earlier zones. Augmenting convective heating with infrared radiation overcomes the cooling effect and leads to higher drying rates. However, optimization of the operating conditions and the residence time in each zone was not considered in their work. Aust et al.[6] also did not perform optimization of operating conditions, but they did show that lower air flow rates are required at higher air temperatures to prevent blister formation.

For a given coating configuration (i.e., coating thickness and initial solvent concentration) and residence time, Price and Cairncross[7] optimized the operating conditions in a single-zone dryer. They defined two objective functions in their formulation of the optimization problem: one minimized the residual solvent, and the other minimized the difference between the maximum solvent partial pressure and the ambient pressure during drying. The second objective function ensured that the coating temperature became almost equal to the bubble-point temperature at some time during drying. With this approach, they found that the optimum heat-transfer coefficients on the coating side (or top side) were always higher than or equal to those on the web side (or bottom side). Their results contradicted the prevalent back-side-drying approach, which suggests that the air flow (or heat-transfer coefficient) on the bottom side should be higher. It was shown that optimum air flows, reported as heat-transfer coefficients, were lower for higher air temperatures; that thicker coatings and coatings with higher solids contents needed to be dried at lower temperatures and higher air flows; and that shorter dryers needed higher air flows.

Alsoy[19] modeled the drying behavior of polymeric coatings in single-zone and multizone dryers. As in earlier reports, it was found that high air flows lead to blister formation in coatings dried in a single-zone dryer. Drying the same coating in a two-zone dryer with a low air flow in the first zone and a high air flow in the second zone prevented blisters and also lowered the residual solvent—a benefit of drying coatings in multizone dryers. It was illustrated that, for a constant total time of drying, more solvent could be removed from a coating when it was dried in eight zones than when it was dried in two zones. The top- and bottom-side air flows at the entrance of each zone of the eight-zone dryer were gradually incremented to avoid blisters. It was further shown that, in the eight-zone dryer, raising the residence time in each subsequent zone rather than having equal residence times in all zones resulted in lower residual solvent than having equal-sized zones. In that study, however, the residence times were adjusted somewhat arbitrarily, and the results were predicted without optimization.

Pourdarvish et al.[20] showed through benchtop experiments that blisters or bubbles can be generated in coatings at temperatures well below the bubble-point temperature—even at room temperature. They observed that bubbles formed when either the air flow or the air temperature was raised. It was hypothesized that blisters formed when the coating became supersaturated with air during drying; degassing the solution prior to casting reduced the propensity of blister formation. The solubility of air in coatings is high when the coatings are applied because of their high solvent content, and as the solvent departs during drying, its concentration, and hence the solubility of air, decreases, leading to saturation and blisters. In the current article, however, we do not consider the effect of dissolved air, recognizing that dissolved air produces blisters at milder operating conditions than does boiling.

Khandelwal et al.[21] optimized operating conditions in a single-zone dryer for two-layer coatings. They formulated an optimization problem equivalent to that of Price and Cairncross.[7] Instead of minimizing two objective functions, however, they minimized only one, which was the residual solvent. The pressure condition was imposed as a constraint that was tantamount to equating the bubble-point temperature and the coating temperature at some time during drying. They found that the heat-transfer coefficients on the bottom side were always greater than or equal to those on the top side, which was opposite to the results reported by Price and Cairncross.[7]

In this article, a short and easy method is developed to obtain near-optimum operating conditions in a single-zone dryer for a given coating configuration and residence time. It has been observed that the convergence of optimization routines for such problems is difficult to achieve and is sensitive to the starting values of the decision variables. In contrast, the simple method presented here requires only the drying code and does not need an optimization routine, and it can be easily used by practicing engineers. To verify the effectiveness of the easy method, its results were compared to those determined using a rigorous method. Our past experience has shown that it is exceedingly difficult for the optimization routine for two-zone dryers to converge. For multizone dryers, convergence would be even more difficult. Therefore, the easy method was used to optimize the operating conditions and residence time in each zone of a three-zone dryer and a four-zone dryer.

For a multizone dryer, the optimization problem involves minimizing the residual solvent at the end of the last zone by varying the operating conditions in all zones for a given initial coating configuration and set of residence times in each zone. The number of operating conditions to be minimized would be twice the number of zones because each zone has two air flows, one on the top of the coating and the other on the bottom; in addition to the operating conditions, the residence time in each zone would also need to be optimized.

The results for multizone dryers obtained using the simple method showed that air flow on the bottom side of the coating should be higher than or equal to that on the top side in all zones. The minimum residence time in the first zone should be such that the bubble-point temperature of the coating starts to rise toward the end of the zone. For three- and four-zone dryers with a fixed total residence time, the residence times in the

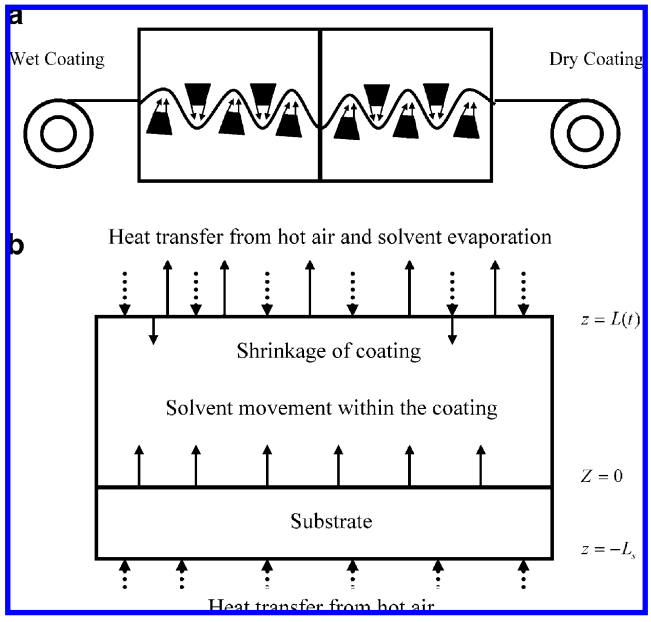

Figure 1. (a) Schematic of an industrial two-zone dryer. Wet coating enters at one end, passes through both zones, and emerges as dry coating. Multizone dryers look similar to two-zone dryers, with each zone operated at a different air flow and temperature. (b) Hot air is blown over the coating and supplies heat to the coating from the top and bottom sides. As the solvent departs into the air from the coating, it shrinks.

second, third, and fourth zones could be varied over a reasonable range to obtain a coating with low residual solvent and no blisters.

Governing Equations

Figure 1a shows a schematic of an industrial dryer in which jets of hot air impinge on a coating moving through a two-zone dryer. A typical dryer has multiple zones, with each zone operated at a different air flow and temperature. Figure 1b depicts several phenomena happening during the drying of a coating. Heat is transferred from the hot air to the top and bottom sides of the coating. Mass is transferred to the air only from the top because the substrate is impermeable. As the solvent departs, the coating shrinks.

Mass Transport. During drying of a coating, both concentration and stress gradients contribute to mass transfer. In-plane stress develops in a drying coating below the glass transition, because the coating cannot shrink in the lateral direction.[22] In this work, poly(vinyl acetate)−toluene system was chosen because its diffusional properties are well-characterized. Poly(vinyl acetate) has a glass transition temperature of about 32 °C, and the coating temperature was always higher than this temperature. During a brief period in the initial stage of drying, the coating temperature was between 25 and 30 °C, but the solvent depressed the glass transition well below 32 °C in this stage. Hence, the stress-driven mass transfer was negligible and was neglected.

Fick's law of diffusion describes solvent mass transport inside the coating. The solvent flux at any point inside the coating is proportional to the gradient of solvent concentration there. The reference velocity to describe mass transfer was chosen as the volume-average velocity because this velocity has been shown to be zero everywhere in a coating at all instants of time if the volumes of the solvent and the polymer are additive.[16] The advantage of choosing the volume-average velocity is that the mass transfer due to convection is zero, so that its contribution need not be included in the mass conservation equation.

By applying solvent mass balance over a differential element, invoking Fick's law to describe the mass flux and letting the size of the element approach zero, we obtained the following partial differential equation for the solvent concentration

$$\frac{\partial c}{\partial t} = \frac{\partial}{\partial z}\left(D\,\frac{\partial c}{\partial z}\right) \tag{1}$$

where c is the concentration of the solvent, t is the time, D is the mutual diffusion coefficient, and z is the distance from the bottom of the coating.

The free-volume theory of Vrentas and Duda[14,15] predicts the mutual diffusion coefficient, D, which is a strong function of temperature and concentration. The theory combines the self-diffusion coefficient and a thermodynamic factor to estimate the mutual diffusion coefficient

$$D = D_0[(1-\varphi_s)^2(1-2\chi\varphi_s)]\exp\left(-\frac{E}{RT}\right)\times \exp\left(-\frac{w_s\hat{V}_s^* + \xi w_p \hat{V}_p^*}{V_{FH}/\gamma}\right) \tag{2}$$

In eq 2, D_0 is the pre-exponential factor, the term within square brackets is the thermodynamic factor, φ_s is the volume fraction of solvent, χ is the interaction parameter in Flory−Huggins theory, E is the activation energy required for diffusion, and T is the temperature. The numerator in the second exponential term is the free volume required for diffusion, and the denominator in this term is the available free volume for diffusion. w_s and w_p are the mass fractions of the solvent and the polymer, respectively. $\hat{V}_s^*$ and $\hat{V}_p^*$ are the specific hole free volumes of the solvent and the polymer, respectively, required for a diffusion jump, and ξ is the ratio of the molar volume of the solvent to that of the polymer. The hole free volume is

$$\frac{V_{FH}}{\gamma} = \frac{K_{11}w_s}{\gamma}(K_{21} - T_{gs} + T) + \frac{K_{12}w_p}{\gamma}(K_{22} - T_{gp} + T) \tag{3}$$

where K_{11}/γ and $(K_{21} - T_{gs})$ are free-volume parameters of the solvent and K_{12}/γ and $(K_{22} - T_{gp})$ are free-volume parameters of the polymer. At low solvent concentrations, D rises several decades with increasing solvent concentration and temperature; at high concentrations, it does not change appreciably with concentration but rises significantly with temperature.

Hong[23] provided free-volume parameters of several solvents and polymers and explained methods to estimate to them. Price et al.[11] mentioned that, of the total of nine parameters [D_0, E, ξ, K_{11}/γ, $(K_{21} - T_{gs})$, K_{12}/γ, $(K_{22}-T_{gp})$, $\hat{V}_s^*$, $\hat{V}_p^*$] required to predict the diffusion coefficient, five [E, K_{11}/γ, $(K_{21} - T_{gs})$, $\hat{V}_p^*$, and $\hat{V}_s^*$] can be calculated from the pure-substance properties, and the remaining four parameters [D_0, ξ, K_{12}/γ, and $(K_{22} - T_{gp})$] can be estimated from drying experiments. They estimated these four parameters by minimizing the difference between experimental weight-loss measurements and predicted values for the poly(vinyl acetate)−toluene system. The estimated properties and those reported by Hong[23] sometimes vary by as much as ~40%. Hence, the data for the system estimated by Price et al.[11] were considered for model predictions in this work. The free-volume parameters of the system are listed in Table 1.[7]

Uniform concentration of the solvent in the coating was employed as the initial condition for eq 1. This equation also needs two boundary conditions: one at the top and the other at

Table 1. Physical Properties and Free-Volume-Theory Parameters for the Poly(vinyl acetate)−Toluene System[7]

Toluene Properties	
ρ_s	0.866 g cm^{-3}
C_{ps}	1.84 J g^{-1} °C^{-1}
M_s	92.14 g mol^{-1}
A	6.95334
B	1343.943
C	219.377
χ	0.39
$\Delta H_{vap\ solvent}$	413.36 J g^{-1}
Poly(vinyl acetate) Properties	
ρ_p	1.17 g cm^{-3}
C_{pp}	1.46 J g^{-1} °C^{-1}
Substrate Properties	
$\rho_{substrate}$	1.38 g cm^{-3}
$C_{p\ substrate}$	1.88 J g^{-1} °C^{-1}
thickness	3.556 × 10^{-3} cm
Diffusion Parameters	
D_0	3.998 × 10^{-4} cm^2 s^{-1}
E_a	0.0 J mol^{-1}
ξ	0.958
K_{11}/γ	2.21 × 10^{-3} cm^3 g^{-1} °C^{-1}
$K_{21} - T_{gs}$	−376 °C
K_{12}/γ	6.145 × 10^{-4} cm^3 g^{-1} °C^{-1}
$K_{22} - T_{gp}$	−496.9 °C
$\hat{V}_s^*$	0.917 cm^3
$\hat{V}_p^*$	1.0 cm^3

the bottom. The solvent mass flux at the bottom ($z = 0$) is zero because the substrate is impermeable. This implies that the concentration gradient of the solvent is zero there because the diffusion coefficient cannot be zero. The solvent flux at the top [$z = z(t)$] can be characterized by a mass-transfer coefficient

$$-D\frac{dc}{dz} + c\frac{dL}{dt} = -k_g(P_S^G - P_S^{G\infty}) \quad (4)$$

where k_g is the mass-transfer coefficient, which was estimated from the known heat-transfer coefficient using the Chilton−Colburn analogy. As mentioned earlier, heat-transfer coefficient is reported as the operating condition for air flow. In eq 4, P_S^G and $P_S^{G\infty}$ are the partial pressures of the solvent at the coating−air interface on the air side and in the bulk air, respectively. The latter was set to zero because evaporation of the solvent does not raise its concentration in air appreciably. P_S^G is the product of the vapor pressure and activity of the solvent at the coating−air interface, which can be obtained from Flory−Huggins theory as

$$P_S^G = P_{sat}\varphi_s \exp(\varphi_p + \chi\varphi_p^2) \quad (5)$$

P_{sat} was estimated by the Antoine equation

$$\log P_{sat} = A - \frac{B}{T + C} \quad (6)$$

where A, B, and C are the Antoine constants listed in Table 1 and φ_p is the volume fraction of the polymer. Equations 1−6 were used to describe mass transport in all zones of the dryer. The heat-transfer coefficient, and thus the mass-transfer coefficient, changed from zone to zone.

Shrinkage of the Coating. A coating shrinks as solvent departs during drying. The rate of shrinkage is determined by the rate of evaporation

$$\frac{dL}{dt} = -k_g\hat{V}_s(P_S^G - P_S^{G\infty}) \quad (7)$$

where $\hat{V}_s$ is the specific volume of the solvent. Equation 7 was obtained by writing the solvent mass balance.

Energy Transport. In a dryer, the coating is heated from both the top and bottom sides. The dominant mode of heat transfer is convection from the air to the coating. A few articles[5,7] have considered the variation of the temperature through the thickness of the coating, and a few[17,24] have ignored it. In this work, the temperature variation through the thickness was neglected because the conductive resistance was assumed to be small compared to convective resistance. Results from our group have shown an insignificant difference in predictions between models that included temperature change and those that ignored it. The expression used for energy transport in this work is

$$(L_sC_{ps}\rho_s + LC_{pc}\rho_c)\frac{dT}{dt} = h_{top}(T_{air} - T) + h_{bottom}(T_{air} - T) - \Delta H_v\dot{m} \quad (8)$$

where h_{top} and h_{bottom} represent heat-transfer coefficients on the top and the bottom sides of the coated substrate, respectively; $\dot{m}$ is the rate of evaporation, which is determined from the right-hand side of eq 7; ΔH_v is the latent heat of vaporization; L, C_p, and ρ stand for thickness, specific heat, and density, respectively; and subscripts s and c indicate the substrate and the coating, respectively. These and other physical properties are listed in Table 1. Convective heat transfer from the air to the coating is determined by the first two terms on right-hand side of eq 8; the third term accounts for heat loss because of evaporation.

Solution of the Equations. Equation 1, a partial differential equation, and eqs 7 and 8, ordinary differential equations, are coupled and nonlinear. Together, they form the governing equations for mass and heat transport during drying in all zones of a dryer. They were solved using Galerkin's method of finite elements, which transforms them into ordinary differential equations. The elements were made nonuniform with their size rising gradually from the top to the bottom. The elements near the top were chosen to be small to capture the precipitous drop in concentration there. The function $r_i = (i - 1/n)^2L(t)$, where i varies from 1 to $n + 1$, n is the number of elements, and $L(t)$ is the coating thickness at any given time, stretched the elements from the top to the bottom of the coating. The size of element i can be obtained by $r_{i+1} - r_i$. The exponent in the stretching function can be changed to raise or lower stretching. The set of ordinary differential equations generated by Galerkin's method was integrated by a stiff solver, ode15s, of MATLAB. A typical run on a 2.66-GHz computer with a memory of 506 MB took about 20 s. A choice of 25 elements made the results independent of the number of elements.

Optimization. As explained in the Introduction, a tradeoff exists between removing the solvent quickly and producing dried coatings without blisters. Intense operating conditions lead to quick removal of the solvent but can create blisters; mild conditions do not induce blisters but decrease the solvent removal rates. Optimum conditions fall between the intense and mild extremes.

To determine the optimum drying conditions (air flow rates on the top and bottom sides and air temperature), an objective function was defined, along the same lines as Price and Cairncross,[7] to minimize the residual solvent at the end of drying

$$\text{objective function} = \int_0^L c_s\,dz \quad (9)$$

where L is the thickness of the coating, which changes with time.

The condition for preventing blister formation was imposed as a constraint. The maximum solvent partial pressure during drying was made equal to the ambient pressure at sometime during drying. This condition is tantamount to making the coating temperature equal to the bubble-point temperature.

The built-in optimization solver fmincon of MATLAB was used to find optimum operating conditions. The criteria for fmincon to converge were default values of 1×10^{-6} for absolute tolerances for residual solvent, pressure constraint, and heat-transfer coefficients. For a given coating configuration, air temperature, and residence time, the solver was used to find the optimum heat-transfer coefficients on the top and bottom sides. As in earlier works, these coefficients are reported for air flows. Correlations can be used to convert the heat-transfer coefficients to air flow rates.

Results and Discussion

Single-Zone Dryer. Khandelwal et al.[21] found that the optimum heat-transfer coefficients for single-zone dryers, on both the top and bottom sides, are lower at higher air temperatures. At all temperatures, the coefficient on the top side was found to be lower than that on the bottom side—this contradicts reported results.[7] Even though the heat- and mass-transfer rates are coupled at the top, higher heat- and mass-transfer coefficients there do not lead to higher overall drying rates.

They[21] explained their results by plotting drying rates as a function of time for two cases: For one case, the optimum heat-transfer coefficients used for the plot were obtained by solving the optimization problem for a given coating configuration, air temperature, and residence time; for the other, the optimum coefficients of the first case were interchanged, making the top-side coefficient higher than the bottom-side one. The sum of the coefficients for the second case was the same as that for the first case. The drying rates were high during initial stages with higher top-side air flows, but they soon plummeted. The rapid fall in drying rate is because of the precipitous decrease in diffusion coefficient due to very low solvent concentration at the top. Drying rates with lower top-side air flows were low in the initial stages; they rose subsequently and remained significantly high for a long period before falling, again because of the low concentration at the top. The result is that the overall drying rate was higher with low top-side air flow and, eventually, less solvent was retained in a coating dried with low air flow on the top.

Intrigued by the above finding, the following analysis was made: At a given air temperature, coating configuration, and residence time, optimum top-side and bottom-side heat-transfer coefficients were obtained by solving the optimization problem. Then, the drying code was run with their values varied in such a way that their sum was equal to the sum of the optimum coefficients determined. It was observed that the coating temperature almost approached the bubble-point temperature for all combinations of the coefficients and the residual solvent decreased with decreasing top-side coefficient. In fact, the residual solvent was lowest when the top-side coefficient was made the lowest allowable value, which sometimes equaled the lowest practical limit of 8.36 W/(m^2 K) and sometimes higher than the limit. In other words, for the same rates of energy delivery (keeping the sum of the coefficients same), the residual solvent was lowest when the air flow rate on the top side was lowest.

Based on the above analysis, an easy method was developed to determine optimum heat-transfer coefficients. For a given coating configuration, air temperature, and residence time, both the heat-transfer coefficients were made low and equal; both were raised in small and equal increments until the coating temperature became equal to the bubble-point temperature. Then, the following approach was adopted to determine near-optimum heat-transfer coefficients:

If $h_{top} + h_{bottom} > 1.5 \times 10^2$ W/(m^2 °C) (the upper practical limit on the heat-transfer coefficients), then set

$$h_{bottom} = 1.5 \times 10^2 \text{ W/(m}^2\text{ °C)}$$

and

$$h_{top} = h_{top} + h_{bottom} - 1.5 \times 10^2 \text{ W/(m}^2\text{ °C)}$$

If $h_{top} + h_{bottom} < 1.5 \times 10^2$ W/(m^2 °C) (the upper practical limit on the heat-transfer coefficients), then set

$$h_{top} = 8.36 \times 10^2 \text{ W/(m}^2\text{ °C)}$$

(the lower practical limit on the heat-transfer coefficients) and

$$h_{bottom} = h_{top} + h_{bottom} - 8.36 \text{ W/(m}^2\text{ °C)}$$

The above method ensures that the top-side coefficient is set to the lowest possible value for a given sum of the coefficients. This minimizes the residual solvent for a given rate of energy delivery. One benefit of this analysis is that near-optimum coefficients can be determined by using the drying code only. There is no need to run an optimization routine whose convergence is difficult to achieve and that is also sensitive to the initial values of the decision variables.

Table 2 lists the top-side and bottom-side heat-transfer coefficients and residual solvent obtained by solving the rigorous optimization problem and those found by the easy method described above. The coefficients determined by the two

Table 2. Comparison of Top- and Bottom-Side Heat-Transfer Coefficients and Residual Solvent Obtained by Easy and Rigorous Methods

air temperature (°C)	h_{top} [W/(m^2 °C)]		h_{bottom}, [W/(m^2 °C)]		residual solvent ($\times 10^3$ g/cm^2)	
	easy method	rigorous method	easy method	rigorous method	easy method	rigorous method
110	150.48	150.48	150.48	150.48	2.2658	2.2658
111	150.48	150.48	150.48	150.48	2.2264	2.2264
112	150.48	150.48	150.48	150.48	2.1875	2.1875
113	150.48	150.48	150.48	150.48	2.1491	2.1491
114	138.78	136.83	146.30	150.48	2.1148	2.1127
118[a]	8.36[a]	8.36[a]	125.40[a]	127.35[a]	1.8417[a]	1.8356[a]
120	8.36	8.36	96.14	97.56	1.8646	1.8589
122	8.36	8.36	75.24	77.86	1.9095	1.8903
124	8.36	8.36	63.54	63.80	1.9364	1.9348
126	8.36	8.36	52.25	53.12	1.9993	1.9872
128	8.36	8.36	42.85	44.50	2.0953	2.0629
130	8.36	8.36	37.62	37.72	2.1487	2.1461
132	8.36	8.36	32.19	32.92	2.2439	2.2191
134	8.36	8.36	29.26	29.42	2.2839	2.2776
136	8.36	8.36	26.75	26.66	2.3226	2.3270
138	8.36	8.36	24.24	24.40	2.3787	2.3706
142	8.36	8.36	20.90	20.89	2.4424	2.4431
144	8.36	8.36	19.23	19.47	2.4919	2.4747
146	8.36	8.36	17.97	18.20	2.5225	2.5046
148	8.36	8.36	17.14	17.09	2.5257	2.5298
150	8.36	8.36	15.88	16.08	2.5716	2.5540
152	8.36	8.36	15.05	15.16	2.5874	2.5764
154	8.36	8.36	14.21	14.31	2.6104	2.6005
156	8.36	8.36	13.38	13.54	2.6367	2.6197
158	8.36	8.36	12.79	12.84	2.6415	2.6356
160	8.36	8.36	12.12	12.18	2.6596	2.6528

[a] Conditions providing the global minimum residual solvent.

Table 3. Optimum Heat-Transfer Coefficients in Each Zone of a Three-Zone Dryer as a Function of Residence Time in Each Zone[a]

zone 1, 120 °C				zone 2, 130 °C				zone 3, 140 °C			
time (s)	h_{top} [W/(m^2 °C)]	h_{bottom} [W/(m^2 °C)]	residual solvent ($\times 10^4$ g/cm^2)	time (s)	h_{top} [W/(m^2 °C)]	h_{bottom} [W/(m^2 °C)]	residual solvent ($\times 10^4$ g/cm^2)	time (s)	h_{top} [W/(m^2 °C)]	h_{bottom} [W/(m^2 °C)]	residual solvent ($\times 10^4$ g/cm^2)
10	20.9	150.48	53.78	40	8.36	35.53	10.19	10	8.36	121.22	7.68
				30	8.36	35.53	13.48	20	8.36	46.82	7.47
				20	8.36	35.53	19.38	30	8.36	25.08	7.51
				10	8.36	35.53	31.21	40	8.36	19.23	7.63
20	8.36	104.5	33.64	30	8.36	44.31	9.49	10	8.36	150.48	6.99
				20	8.36	44.31	12.92	20	8.36	48.49	6.83[b]
				10	8.36	44.31	19.53	30	8.36	24.24	6.95
30	8.36	104.5	19.77	20	8.36	79.42	9.37	10	8.36	146.3	6.90
				10	8.36	79.42	12.95	20	8.36	39.29	6.85
40	8.36	104.5	13.51	10	8.36	150.48	9.57	10	8.36	121.22	7.03

[a] Initial coating composition, 30 wt % poly(vinyl acetate)−70 wt % toluene; initial coating thickness, 148 μm; initial coating temperature, 25 °C. [b] Conditions providing minimum residual solvent in zone 3.

methods differed by at most 1%. The heat-transfer coefficients listed for each temperature are local optima. The global optimum temperature is 118 °C because residual solvent is lowest at this temperature. For temperatures lower or higher than the global optimum, the residual solvent rises.

For a more rigorous test, the developed method was also used to determine global optimum coefficients as a function of initial coating thickness and initial coating composition. It was found that the global optimum air temperatures fall and the residual solvent rises with a rise in initial coating thickness; the optimum heat-transfer coefficients, on both the top and bottom sides, rise with coating thickness. It was also observed that the global optimum air temperature rises and the residual solvent falls with a rise in polymer content of the coating; the optimum heat-transfer coefficients fall with an increase in polymer content. These results are in keeping with the results reported by Price and Cairncross[7] with one difference: the coefficient on the top side is lower than that on the bottom side.

Encouraged by the ability of the easy method to predict optimum heat-transfer coefficients, this method was extended to optimize operating conditions in multizone dryers; in such dryers, the residence time in each zone also needs to be optimized. Optimization of multizone dryers involves minimizing the residual solvent at the exit of the last zone by simultaneously varying the heat-transfer coefficients and residence times in all zones. For an n-zone dryer, $2n$ heat-transfer coefficients and $n - 1$ residence times need to be optimized if the total drying time is fixed. This implies eight parameters for a three-zone dryer, 11 for four-zone dryer, and so on.

Convergence for a one-zone dryer is hard to achieve, and that for a multizone dryer would be exceedingly difficult. One way around this problem would be to optimize operating conditions, zone by zone, for fixed residence times. That is, one could optimize heat-transfer coefficients in zone 1 first, followed by zone 2, zone 3, and so on. This means sequential optimization of operating conditions. It has been observed that sequential optimization of a two-zone dryer is also not easy, with severe convergence problems in zone 2.

Easy method described above for single-zone dryers was adopted for optimization of multizone (three- and four-zone) dryers. For a fixed initial coating configuration, air temperature in each zone, and residence time in each zone, optimum heat-transfer coefficients were found for each zone sequentially by using the easy method. The residence time in each zone was varied by either 5 or 10 s, with the total residence time kept constant, and for each set of residence times, optimum heat-transfer coefficients in each zone were determined. The easy method could be used to obtain optimum conditions for any distribution of residence times as well.

Three-Zone Dryer. The easy method was applied to optimize the heat-transfer coefficients and residence time in each zone of a three-zone dryer. The coating had an initial thickness of about 148 μm; 30 wt % polymer; and air temperatures in zones 1, 2, and 3, respectively, set to 120, 130, and 140 °C or 130, 140, and 150 °C. The total residence time was fixed at 60 s. The optimum heat-transfer coefficients were obtained in each zone for several combinations of residence times in the three zones. The coefficients were found sequentially starting with zone 1 and then proceeding to zone 2 followed by zone 3.

Table 3 reports the heat-transfer coefficients and residual solvent amounts at the end of each zone, when the air temperatures were 120, 130, and 140 °C. The residence time in zone 1 was set to 10 s, and those in zones 2 and 3 were changed so that the total residence time was 60 s. The residual solvent at the end of zone 2 was found to increase with decreasing residence time in this zone. The residual solvent at the end of zone 3 goes through a minimum, although the difference between maximum and minimum residual solvent is not significant.

It was observed that the bubble-point temperature did not begin to rise at the end of the first zone for 10-s residence time in that zone. This necessitated slower heating of the coating in the second zone so that the coating temperature did not cross the bubble-point temperature. Hence, the heat-transfer coefficients on both sides in zone 2 are low and insensitive to residence time in that zone. In the third zone, however, the heat-transfer coefficient on the bottom side increases as the zone becomes shorter. This is because the bubble-point temperature rises throughout the second zone and higher heat-transfer coefficients (or air flows) are needed in the third zone to force the coating temperature to become equal to the bubble-point temperature. The shorter the third zone, the higher the heat-transfer coefficients needed to ensure equality.

When the residence time in the first zone was raised to 20 s, the heat-transfer coefficients in the second zone were higher than those corresponding to the residence time of 10 s in the first zone. Again, the second-zone heat-transfer coefficients were almost independent of residence time in the second zone because of the small rise in the bubble-point temperature at the end of the first zone. Similar observations were made for a residence time of 30 s in the first zone.

The residence time in zone 1 was changed to 20, 30, and 40 s, and those in zones 2 and 3 were varied such that the total residence time was 60 s. The global minimum was found when the residence times in the first, second, and third zones were 20 s each. It is to be noted that the operating conditions and the residence times found would represent a near-global optimum because the residence times were changed in incre-

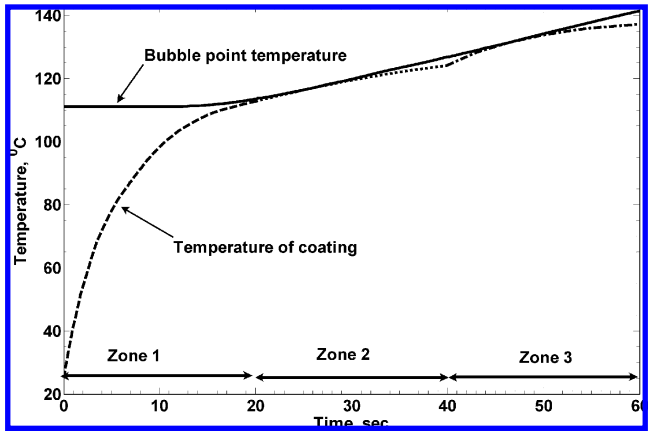

Figure 2. Evolution of coating temperature and bubble-point temperature in each zone of a three-zone dryer. The initial coating composition was 30 wt % poly(vinyl acetate)−70 wt % toluene. The initial coating thickness was about 148 μm, and the initial coating temperature was 25 °C. The first-, second-, and third-zone air temperatures were 120, 130, and 140 °C, respectively.

ments of 5 or 10 s. For other combinations of residence times, the residual solvent at the end of the third zone changed slightly. For example, with residence times of 20, 30, and 10 s, the residual solvent was close to the minimum value. Similarly, for several other combinations, the residual solvent at the end of the third zone did not deviate much from the minimum value. Even with a residence time of 30 s in the first zone and two combinations of times in zones 2 and 3, the residual solvent at the end of the third zone did not change much from the minimum value.

It was observed that the bubble-point temperature started to rise at about 13 s for all residence times considered in Table 3 for the first zone. Generally, it rose later if the residence time was increased. It is expected that the optimum residence time in the first zone would be close to 13 s, preferably higher than this value, but not necessarily. If it were far lower than 13 s, the coating could not be heated at high air flows in the second zone. Otherwise, blisters would form in the coating. If it were far higher than 13 s, the coating would have spent more time in the first zone and less time in subsequent zones, which are operated at higher temperatures, leading to higher residual solvent at the end of zone 3. A residence time of 20 s in the first zone resulted in minimum residual solvent at the end of third zone because increments of 10 s were considered in Table 3 (some time between 13 and 20 s could also lead to lower residual solvent). If the residence time in the first zone were too long (40 s), the air flows in the second zone would rise, and the residual solvent at the end of this zone would be lower, but the final residual solvent would be higher because the coating would not be dried for sufficient time in the third zone.

Figure 2 shows the coating and bubble-point temperatures for the combination of residence times (i.e., 20 s in each zone) that gives the minimum residual solvent at the end of the third zone. It can be observed that the bubble-point temperature starts rising toward end of the first zone and it rises faster thereafter. In each zone, the coating temperature approaches the bubble-point temperature within a certain tolerance. When the residence time in the first zone is either too short or too long compared to 20 s, the residual solvent seems to be rising. When the residence time in the first zone is 10 s, the residual solvent at the end of the third zone rises considerably. If it is close to 20 s, the residual solvent changes insignificantly. It appears that the length of the first zone should be such that the bubble-point temperature should start rising toward the end of this zone. The lengths of the second and third

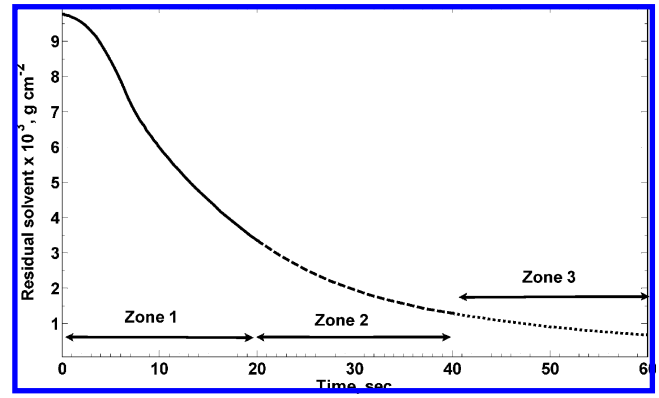

Figure 3. Evolution of residual solvent in a three-zone dryer for the poly(vinyl acetate)−toluene system. The initial coating composition was 30 wt % poly(vinyl acetate)−70 wt % toluene, the initial coating thickness was about 148 μm, and the initial coating temperature was 25 °C. The first-, second-, and third-zone air temperatures were 120, 130, and 140 °C, respectively.

zones could then be changed reasonably to obtain near-optimum residual solvent at the end of the third zone.

Figure 3 shows the residual solvent as a function of time for the three-zone dryer. It decreases continuously without any sudden drop as the coating enters the second and third zones. This is because of the lower rate of heating and the small rise in air temperature from zone to zone.

Table 4 shows data similar to those in Table 3 for the same initial coating configuration. The air temperatures in the three zones were changed to 130, 140, and 150 °C, respectively. The near-optimum heat-transfer coefficients were lower than those in Table 3 because of higher air temperatures in each zone. It was found that the bubble-point temperature started to rise in the first zone if the residence time there was at least 11 s. Hence, the residence time in the first zone should be close to 11 s. The residual solvent at the end of the third zone was lowest when the residence time in zone 1 was 10 s. For this set of temperatures, the bubble-point temperature started to rise sooner than for the temperatures in Table 3; therefore, the first zone became shorter. The residual solvent at the end of the third zone was insensitive to the residence times in the second and third zones if the residence time in the first zone was fixed at 10 s. If the first zone was too short (5-s residence time) or too long (30-s residence time), the residual solvent at the end of the third zone rose considerably. Hence, the residence time in the first zone should be close to 10s. The residence times in the second and third zones could be changed reasonably as long as they were sufficiently long. Similarly to Figure 2, it was found that the coating temperature approached the bubble-point temperature in all three zones. The residual solvent fell without any sudden drop at the entrances of the second and third zones.

Table 5 shows data similar to those in Table 3. All conditions were the same as for Table 3, except for the initial coating thickness, which was reduced to 112 μm. As expected, the residual solvent at the end of third zone was less than that with 148-μm initial thickness. The bubble-point temperature started rising at about 6 s; hence, the residence time in the first zone should be close to 6 s. However, the residence times in the first, second, and third zones for minimum residual solvent at the end of the third zone were found to be 20, 10, and 30 s, respectively. A combination of 15, 15, and 30 s for the residence times in the first, second, and third zones, respectively, also gave a residual solvent at the end of the third zone that was very close to the minimum value. It is not clear why the best residence time in the first zone is far higher than 6 s. In fact,

Table 4. Optimum Heat-Transfer Coefficients in Each Zone of a Three-Zone Dryer as a Function of Residence Time in Each Zone[a]

zone 1, 130 °C				zone 2, 140 °C				zone 3, 150 °C			
time (s)	h_{top} [W/(m^2 °C)]	h_{bottom} [W/(m^2 °C)]	residual solvent ($\times 10^4$ g/cm^2)	time (s)	h_{top} [W/(m^2 °C)]	h_{bottom} [W/(m^2 °C)]	residual solvent ($\times 10^4$ g/cm^2)	time (s)	h_{top} [W/(m^2 °C)]	h_{bottom} [W/(m^2 °C)]	residual solvent ($\times 10^4$ g/cm^2)
5	79.42	150.48	68.06	5	8.36	19.86	51.32	50	8.36	10.45	7.82
				10	8.36	18.68	39.68	45	8.36	10.24	7.84
				15	8.36	18.64	30.75	40	8.36	10.24	7.82
				20	8.36	18.64	24.23	35	8.36	10.03	7.83
				25	8.36	18.60	19.58	30	8.36	10.41	7.81
				30	8.36	18.56	16.21	25	8.36	11.79	7.78
				35	8.36	18.64	13.69	20	8.36	14.80	7.74
				40	8.36	18.52	11.78	15	8.36	19.94	7.78
				45	8.36	18.64	10.25	10	8.36	28.00	7.84
				50	8.36	18.52	9.05	5	8.36	47.40	7.95
10	8.36	118.29	55.27	40	8.36	19.81	8.99	10	8.36	39.92	6.68
				30	8.36	19.81	12.29	20	8.36	19.60	6.56[b]
				20	8.36	19.86	19.26	30	8.36	13.13	6.61
				10	8.36	19.86	30.57	40	8.36	12.08	6.64
20	8.36	63.95	36.52	30	8.36	21.15	9.46	10	8.36	33.73	6.90
				20	8.36	21.19	13.31	20	8.36	16.93	6.85
				10	8.36	21.19	20.72	30	8.36	12.54	6.92
30	8.36	51.04	22.53	20	8.36	21.07	9.85	10	8.36	30.51	7.15
				10	8.36	21.74	14.09	20	8.36	15.55	7.09

[a] Initial coating composition, 30 wt % poly(vinyl acetate)−70 wt % toluene; initial coating thickness, 148 μm; initial coating temperature, 25 °C. [b] Conditions providing minimum residual solvent in zone 3.

Table 5. Optimum Heat-Transfer Coefficients in Each Zone of a Three-Zone Dryer as a Function of Residence Time in Each Zone[a]

zone 1, 120 °C				zone 2, 130 °C				zone 3, 140 °C			
time (s)	h_{top} [W/(m^2 °C)]	h_{bottom} [W/(m^2 °C)]	residual solvent ($\times 10^4$ g/cm^2)	time (s)	h_{top} [W/(m^2 °C)]	h_{bottom} [W/(m^2 °C)]	residual solvent ($\times 10^4$ g/cm^2)	time (s)	h_{top} [W/(m^2 °C)]	h_{bottom} [W/(m^2 °C)]	residual solvent ($\times 10^4$ g/cm^2)
5	140.97	150.48	45.15	5	8.36	46.40	27.28	50	8.36	31.48	2.82
				10	8.36	46.40	17.90	45	8.36	38.87	2.76
				15	8.36	46.40	12.74	40	8.36	55.64	2.71
				20	8.36	46.40	9.72	35	8.36	94.84	2.69
				25	8.36	46.40	7.80	30	8.36	150.48	2.73
				30	8.36	46.52	6.48	25	8.36	150.48	2.84
				35	8.36	46.40	5.52	20	8.36	150.48	2.95
				40	8.36	46.40	4.80	15	8.36	150.48	3.07
				45	8.36	46.40	4.24	10	8.36	150.48	3.20
				50	8.36	46.40	3.79	5	8.36	150.48	3.33
10	30.60	150.48	28.71	10	8.36	55.47	12.40	40	8.36	55.26	2.47
				20	8.36	55.51	7.31	30	8.36	150.48	2.49
				30	8.36	55.59	5.10	20	8.36	150.48	2.69
				40	8.36	55.59	3.89	10	8.36	150.48	2.92
15	25.08	150.48	18.06	5	8.36	87.40	12.27	40	8.36	44.69	2.48
				10	8.36	87.32	9.01	35	8.36	98.23	2.39[b]
				15	8.36	87.22	7.07	30	145.46	150.48	2.39[b]
				20	8.36	87.36	5.80	25	150.48	150.48	2.48
20	25.71	150.48	12.53	10	67.09	150.48	7.05	30	135.43	150.48	2.39[b]
				20	67.88	150.48	4.85	20	150.48	150.48	2.55
				30	68.13	150.48	3.70	10	150.48	150.48	2.76
30	25.67	150.48	7.78	10	150.48	150.48	5.23	20	150.48	150.48	2.67
				20	150.48	150.48	3.92	10	150.48	150.48	2.89
40	25.50	150.48	5.71	10	150.48	150.48	4.21	10	150.48	150.48	3.06

[a] Initial coating composition, 30 wt % poly(vinyl acetate)−70 wt % toluene; initial coating thickness, 112 μm; initial coating temperature, 25 °C. [b] Conditions providing minimum residual solvent in zone 3.

the residual solvent at the end of third zone for a residence-time combination of 10, 10, and 40 s was close to the minimum value. Our results for several other cases showed that residence time in the first zone should be close to the value for which the bubble-point temperature starts to rise toward the end of the zone.

Table 5 shows that the residual solvent at the end of the third zone is minimized for three combinations of residence times (15, 10, and 35 s; 15, 15, and 30 s; and 20, 10, and 30 s). A unique solution might not be attainable for the multizone optimization problem. For a fixed total residence time in the dryer, different combinations of residence times in individual zones could give the same or nearly the same optimal residual solvent. When the time in zone 2 was raised to 15s, the bubble-point temperature at the exit of zone 2 increased more than it did for a residence time of 10 s. Consequently, the heat-transfer coefficients in zone 3 were higher for a 15-s residence time in zone 2 than for a 10-s zone2 residence time. The residual solvent at the end of third zone did not change, however, because the drying time in this zone was reduced from 35 to 30 s. When the residence time in zone 1 was raised to 20 s, the coating could be dried at high air flows in zones 2 and 3 (compared to the case of a 10-s residence time in zone 1) because of the higher rise in bubble-point temperature. The final residual solvent, however, did not change because the coating was dried for shorter times in zones 2 and 3. The existence of multiple solutions could cause severe convergence problems if rigorous optimization were used. The simple method described in this work, however, eliminates such problems.

Table 6. Optimum Heat-Transfer Coefficients in Each Zone of a Four-Zone Dryer as a Function of Residence Time in Each Zone[a]

zone 1, 130 °C				zone 2, 140 °C				zone 3, 150 °C				zone 4, 160 °C			
time (s)	h_{top} [W/(m^2 °C)]	h_{bottom} [W/(m^2 °C)]	residual solvent ($\times 10^4$ g/cm^2)	time (s)	h_{top} [W/(m^2 °C)]	h_{bottom} [W/(m^2 °C)]	residual solvent ($\times 10^4$ g/cm^2)	time (s)	h_{top} [W/(m^2 °C)]	h_{bottom} [W/(m^2 °C)]	residual solvent ($\times 10^4$ g/cm^2)	time (s)	h_{top} [W/(m^2 °C)]	h_{bottom} [W/(m^2 °C)]	residual solvent ($\times 10^4$ g/cm^2)
10	8.36	120.18	55.27	40	8.36	19.81	8.99	10	8.36	39.92	6.68	20	8.36	18.48	3.79
								20	8.36	39.87	5.04	10	8.36	85.23	3.74
				30	8.36	19.81	12.29	20	8.36	19.62	6.56	20	8.36	29.97	3.68[b]
								10	8.36	19.69	8.81	30	8.36	10.24	3.83
								30	8.36	19.65	5.05	10	8.36	96.22	3.75
				20	8.36	19.86	18.26	30	8.36	13.13	6.61	20	8.36	33.86	3.70
								20	8.36	13.13	8.76	30	8.36	14.30	3.74
								10	8.36	13.13	12.21	40	8.36	7.02	3.93
				10	8.36	19.86	30.57	40	8.36	12.07	6.64	20	8.36	33.98	3.72
								30	8.36	12.07	8.78	30	8.36	15.09	3.7
								20	8.36	12.07	12.19	40	8.36	7.82	3.89
								10	8.36	12.25	18.260	50	8.36	6.27	3.98
20	8.36	63.89	36.49	30	8.36	21.15	9.46	10	8.36	33.73	6.92	20	8.36	17.81	3.86
								20	8.36	33.94	5.17	10	8.36	72.31	3.81
				20	8.36	21.19	13.30	10	8.36	17.01	9.31	30	8.36	9.99	3.92
								20	8.36	16.93	6.85	20	8.36	27.25	3.78
								30	8.36	16.93	5.23	10	8.36	79.42	3.86
				10	8.36	21.19	20.72	30	8.36	12.54	6.92	20	8.36	29.58	3.82
								20	8.36	12.48	9.31	30	8.36	13.10	3.86
								40	8.36	12.46	5.34	10	8.36	76.45	3.96
				40	8.36	21.19	7.16	10	8.36	86.44	5.33	10	8.36	47.65	3.93
30	8.36	51.04	22.53	20	8.36	21.99	9.81	20	8.36	30.10	5.31	10	8.36	63.75	3.90
								10	8.36	30.10	7.12	20	8.36	16.55	3.95
				10	8.36	21.99	14.08	30	8.36	15.47	5.39	10	8.36	69.39	3.97
								20	8.36	15.47	7.08	20	8.36	25.29	3.88
								10	8.36	15.47	9.71	30	8.36	10.14	4.00

[a] Initial coating composition, 30 wt % poly(vinyl acetate)−70 wt % toluene; initial coating thickness, 112 μm; initial coating temperature, 25 °C. [b] Conditions providing minimum residual solvent in zone 4.

In general, the bubble-point temperature is expected to rise sooner for thinner coatings; therefore, the residence time in the first zone becomes shorter. It was found that the bubble-point temperature started rising at about 10 s, which means that the first-zone residence time should be close to 10 s. The data support the conclusions drawn earlier that the minimum residence time in the first zone should be such that the bubble-point temperature begins to rise near the end of this zone. Table 5 also shows that the residence times in the second and third zones are flexible but that neither of them can be made too short or too long.

The intention of this work was to demonstrate the ability of the easy method to find optimum operating conditions and residence times in multizone dryers and not to determine them exactly. For example, the residence times in each zone could be changed systematically in small increments to find those that optimize the dryer operation. The total residence time could be changed to a value other than 60 s, and the method could be used to find near-optimum operating conditions and distributions of residence times in the three zones.

Four-Zone Dryer. The easy method was applied to optimize the heat-transfer coefficients and residence times in each zone of a four-zone dryer. The coating had an initial thickness of about 148 μm; 30% by weight polymer; and air temperatures in zones 1−4 set to 130, 140, 150, and 160 °C, espectively. The total residence time was fixed at 80 s. The optimum heat-transfer coefficients were obtained in each zone for several combinations of residence times in the four zones. The coefficients were found sequentially starting with zone 1.

Table 6 shows the optimum heat-transfer coefficients and residual solvent amounts at the end of each zone for several combinations of residence times in the four zones. The bubble-point temperature began to rise in the first zone if the residence time there was at least 8 s. Hence, the residence time in the first zone should be close to 8 s for minimum residual solvent at the end of zone 4. It was found that the optimum residual solvent at the end of the fourth zone was obtained when the residence times in the four zones were 10, 30, 20, and 20 s, respectively. The residual solvent at the end of fourth zone was insensitive to the residence times in the second, third, and fourth zones as long as each of these zones was reasonably long. Also, the residual solvent at the end of fourth zone did not vary much when the residence time in the first zone was raised to 20 s and the other residence times were changed with the constraint that the total residence time was 80 s. However, the residual solvent at the end of the fourth zone rose significantly when the residence time in the first zone was made far longer (30 s) than 10 s and the others were varied for a total time of 80 s.

Conclusions

Air flows have been nearly optimized in single-zone and multizone dryers by mathematical modeling for a given initial coating configuration and air temperature(s). Residence times have also been nearly optimized for multizone dryers. Optimization was done by minimizing the residual solvent at the end of the last zone with the stipulation that blisters should not be induced in the coating in any zone. These conditions were met by forcing the maximum solvent partial pressure to become equal to the ambient pressure, within a certain tolerance, at some time during drying; this is tantamount to making the coating temperature approach bubble-point temperature at some time during drying in each zone.

Rigorous optimization showed that the air flows on the top side should always be less than or equal to those on the bottom side. It was shown in earlier work that the initial drying rates are high with high air flows on the top side but they soon plummet; with low air flows on the top side, drying rates remain considerably high for longer durations, with the result that the overall drying rates are high. Careful examination of the optimization results under various conditions revealed that, for the same rates of energy delivery, the residual solvent was lowest for the lowest allowable top-side air flow (or heat-transfer coefficient). Based on the examination, an easy method was developed to optimize operating conditions. This method obviated the use of an optimization routine and optimized the conditions with the drying code only. This is a great benefit because the convergence of optimization routines is difficult to achieve and often depends on the starting values for the decision variables.

The easy method was adopted to optimize operating conditions and also residence times in three and four-zone dryers. The use of rigorous optimization for such problems would involve finding 8 and 11 variables for three-zone and four-zone dryers, respectively, for a fixed total residence time. This is a monumental task and would be very difficult to achieve. Optimization was done sequentially zone by zone starting with the first zone.

The results indicate that the residence time in the first zone should be close to the value for which the bubble-point temperature starts to rise toward the end of this zone. The residual solvent at the end of last zone was found to be insensitive to the residence times in the subsequent zones as long as each of these residence times was reasonably long.

Literature Cited

(1) Okazaki, M.; Shioda, K.; Masuda, K.; Toei, R. Drying Mechanism of Coated Film of Polymer Solution. *J. Chem. Eng. Jpn.* **1974**, *7* (2), 99.

(2) Blandin, H. P.; David, J. C.; Vergnaud, J. M.; Illien, J. P.; Malizewicz, M. Modeling of Drying of Coatings: Effect of Thickness, Temperature and Concentration of Solvent. *Prog. Org. Coat.* **1987**, *15*, 163.

(3) Gutoff, E. B. Modeling the Drying of Solvent Coatings on Continuous Webs. *J. Imaging Sci. Technol.* **1994**, *38* (2), 184.

(4) Vrentas, J. S.; Vrentas, C. M. Drying of Solvent Coated Polymer Films. *J. Polym. Sci. B: Polym. Phys.* **1994**, *32* (1), 187.

(5) Cairncross, R. A.; Jeyadev, S.; Dunham, R. F.; Evans, K.; Francis, L. F.; Scriven, L. E. Modeling and Design of an Industrial Dryer with Convective and Radiant Heating. *J. Appl. Polym. Sci.* **1995**, *58* (8), 1279.

(6) Aust, R.; Durst, F.; Raszillier, H. Modeling a Multiple-Zone Air Impingement Dryer. *Chem. Eng. Process.* **1997**, *36* (6), 469.

(7) Price, P. E., Jr.; Cairncross, R. A. Optimization of Single-Zone Drying of Polymer Solution Coatings Using Mathematical Modeling. *J. Appl. Polym. Sci.* **2000**, *78* (1), 149.

(8) Narayan, R.; Duda, J. L. Analysis of a Gap Dryer Used to Produce Polymer Films and Coatings. *AIChE J.* **2001**, *47* (5), 972.

(9) Yapel, R. A. The Physical Model of Drying of Coated Films. M.S. Thesis, University of Minnesota, Minneapolis, MN, 1988.

(10) Saure, R.; Wagner, G. R.; Schlunder, E.-U. Drying of Solvent-Borne Polymeric Coatings. I. Modeling the Drying Process. *Surf. Coat. Technol.* **1998**, *99* (3), 253.

(11) Price, P. E., Jr.; Wang, S.; Romdhane, I. H. Extracting Effective Diffusion Parameters from Drying Experiments. *AIChE J.* **1997**, *43* (8), 1925.

(12) Schabel, W. S.; Scharfer, P. S.; Kind, M. Measurement and Simulation of Concentration Profiles During Drying of Thin Films with Help of Confocal-Micro-Raman Spectroscopy. *Chem.-Ing.-Tech.* **2003**, *75* (8), 1105.

(13) Schabel, W.; Scharfer, P.; Mueller, M.; Ludwig, I.; Kind, M. Measurement and Simulation of Concentration Profiles in the Drying of Binary Polymer Solutions. *Chem.-Ing.-Tech.* **2003**, *75* (9), 1336.

(14) Vrentas, J. S.; Duda, J. L. Diffusion in Polymer−Solvent Systems. I. Reexamination of the Free-Volume Theory. *J. Polym. Sci. B: Polym. Phys.* **1977**, *15*, 403.

(15) Vrentas, J. S.; Duda, J. L. Diffusion in Polymer−Solvent Systems. II. A Predictive Theory for the Dependence of Diffusion Coefficients on

Temperature, Concentration, and Molecular Weight. *J. Polym. Sci. B: Polym. Phys.* **1977**, *15*, 417.

(16) Cairncross, R. A. Solidification Phenomena During Drying of Sol-to-Gel Coatings. Ph.D. Thesis, University of Minnesota, Minneapolis, MN, 1994.

(17) Alsoy, S.; Duda, J. L. Drying of Solvent Coated Polymer Films. *Drying Technol.* **1998**, *16* (1 & 2), 15.

(18) Vinjamur, M. Trapping Skinning: An Anomalous Drying Behavior of Polymer−Solvent Systems. Ph.D. Thesis, Drexel University, Philadelphia, PA, 2001.

(19) Alsoy, S. Predicting Drying in Multiple-Zone Ovens. *Ind. Eng. Chem. Res.* **2001**, *40* (14), 2995.

(20) Pourdarvish, R.; Danner, R. P.; Duda, J. L. Mechanism of Bubble Formation in the Drying of Polymer Films. *J. Appl. Polym. Sci.* **2009**, *111* (1), 417.

(21) Khandelwal, A.; Singhania, M.; Vinjamur, M. Optimization of Operating Conditions in a Single-Zone Drier for Two-Layer Polymer Coatings. *J. Appl. Polym. Sci.* **2009**, *111* (1), 308.

(22) Vinjamur, M.; Cairncross, R. A. Non-Fickian Nonisothermal Model for Drying of Polymer Coatings. *AIChE J.* **2002**, *48* (11), 2444.

(23) Hong, S. Prediction of Polymer/Solvent Diffusion Behavior Using Free-Volume Theory. *Ind. Eng. Chem. Res.* **1995**, *34* (7), 2536.

(24) Alsoy, S.; Duda, J. L. Modeling of Multilayer Drying of Polymer Films. *J. Polym. Sci. B: Polym. Phys.* **1999**, *37* (14), 1665.

Received for review April 15, 2009
Revised manuscript received August 5, 2009
Accepted September 8, 2009

IE900604F